Supplementary Information

Iron-induced demethoxylation of lignin as an important source for methanol and its oxidation products in the environment

Jonas Hädeler[1*#], Gunasekaran Velmurugan[2#], Rebekka Lauer[1], Isabel Hanstein[1], Julia Wenhuda[1], Rejith Radhamani[2], Peter Comba[2,3*] and Frank Keppler[1,4*]

[1] Institute of Earth Sciences, Heidelberg University, INF 234-236, D-69120 Heidelberg, Germany

[2] Anorganisch-Chemisches Institut, Heidelberg University, INF 270, D-69120 Heidelberg, Germany

[3] Universität Heidelberg, Interdisciplinary Center for Scientific Computing, INF 205, D-69120 Heidelberg, Germany

[4] Heidelberg Center for the Environment (HCE), Heidelberg University, D-69120 Heidelberg, Germany

*Correspondence:

Jonas Hädeler: jonas.haedeler@geow.uni-heidelberg.de

Peter Comba: peter.comba@aci.uni-heidelberg.de

Frank Keppler: frank.keppler@geow.uni-heidelberg.de

[#] These authors contributed equally

Table of contents

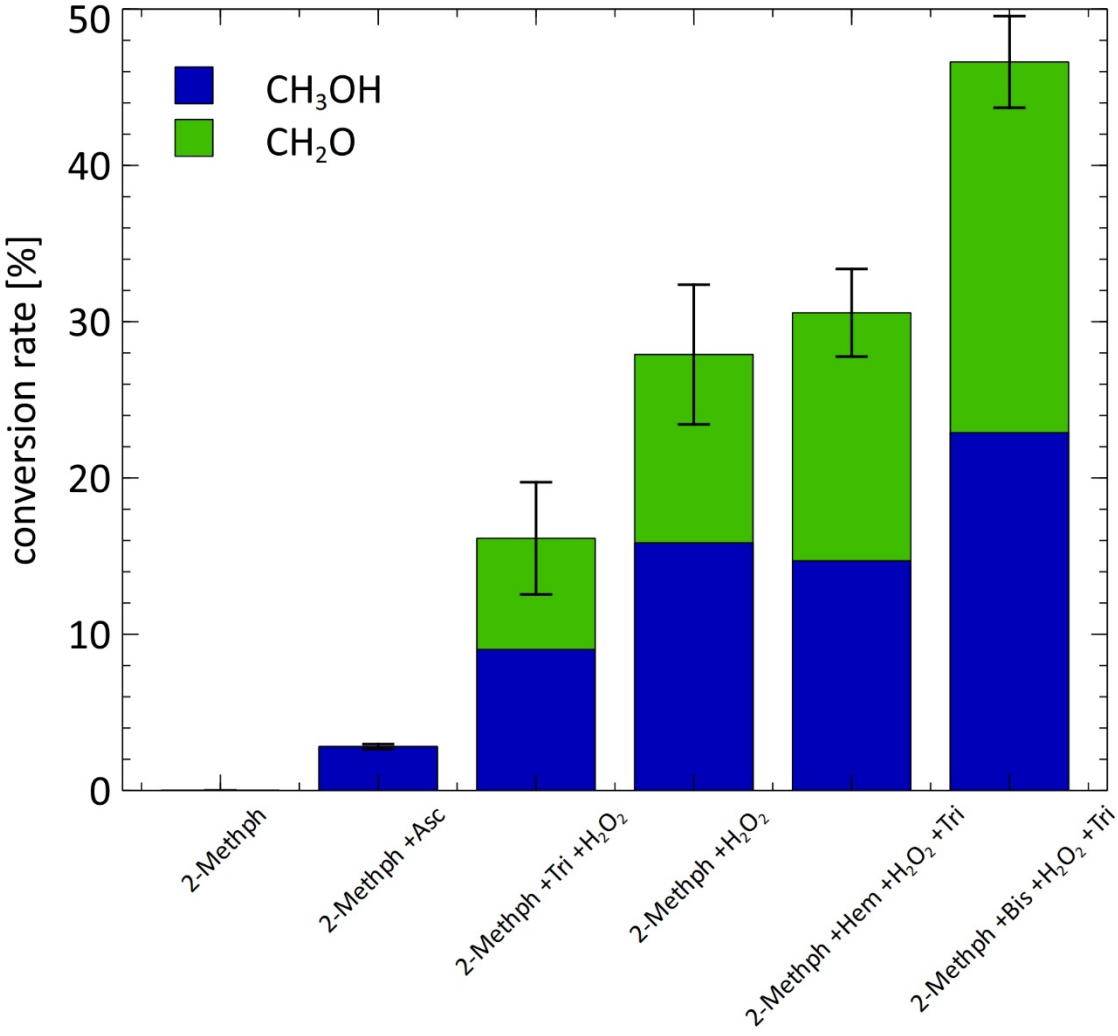

Fig. S1: Conversion rates of 2-methoxyphenol to CH_3OH and CH_2O with different setups of the added iron species, acid, and H_2O_2

Formation of CH_3OH and CH_2O from 2-methoxyphenol in experiments by removing parts of the reactants (10 µmol [(L)$Fe^{II}Cl_2$], or Fe_2O_3, 200 µmol H_2O_2, 100 µmol ascorbic acid, and 0.05 µmol triflic acid). Reactions were performed in 10 mL H_2O. All provided data were evaluated at 22 °C and ambient pressure (1013 mbar) after 48 h reaction time. Conversion rates were related to one methoxy group. Error bars represent the standard deviation of total CH_3OH and CH_2O conversion, based on the mean of three independent experiments (n=3), each measured in triplicate.

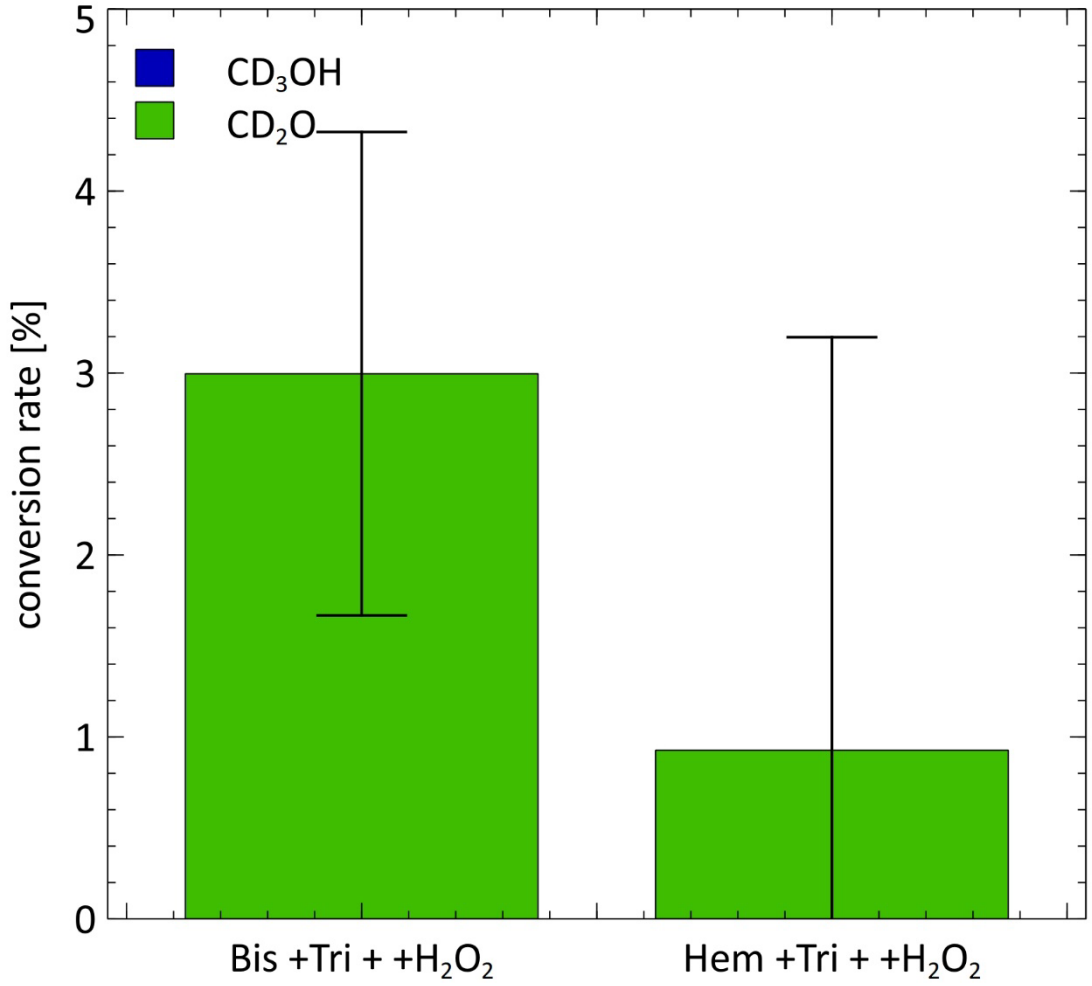

Fig. S2: Conversion rates of phenol to CH_3OH and CH_2O with different iron species, triflic acid, and H_2O_2

Formation of CH_3OH and CH_2O from phenol in experiments mediated 10 µmol [(L)$Fe^{II}Cl_2$], or Fe_2O_3 with 200 µmol H_2O_2, and 0.05 µmol triflic acid. Reactions were performed in 10 mL H_2O. All provided data were evaluated at 22 °C and ambient pressure (1013 mbar) after 48 h reaction time. Conversion rates were related to one methoxy group. Error bars represent the standard deviation of total CH_3OH and CH_2O conversion, based on the mean of three independent experiments (n=3), each measured in triplicate.

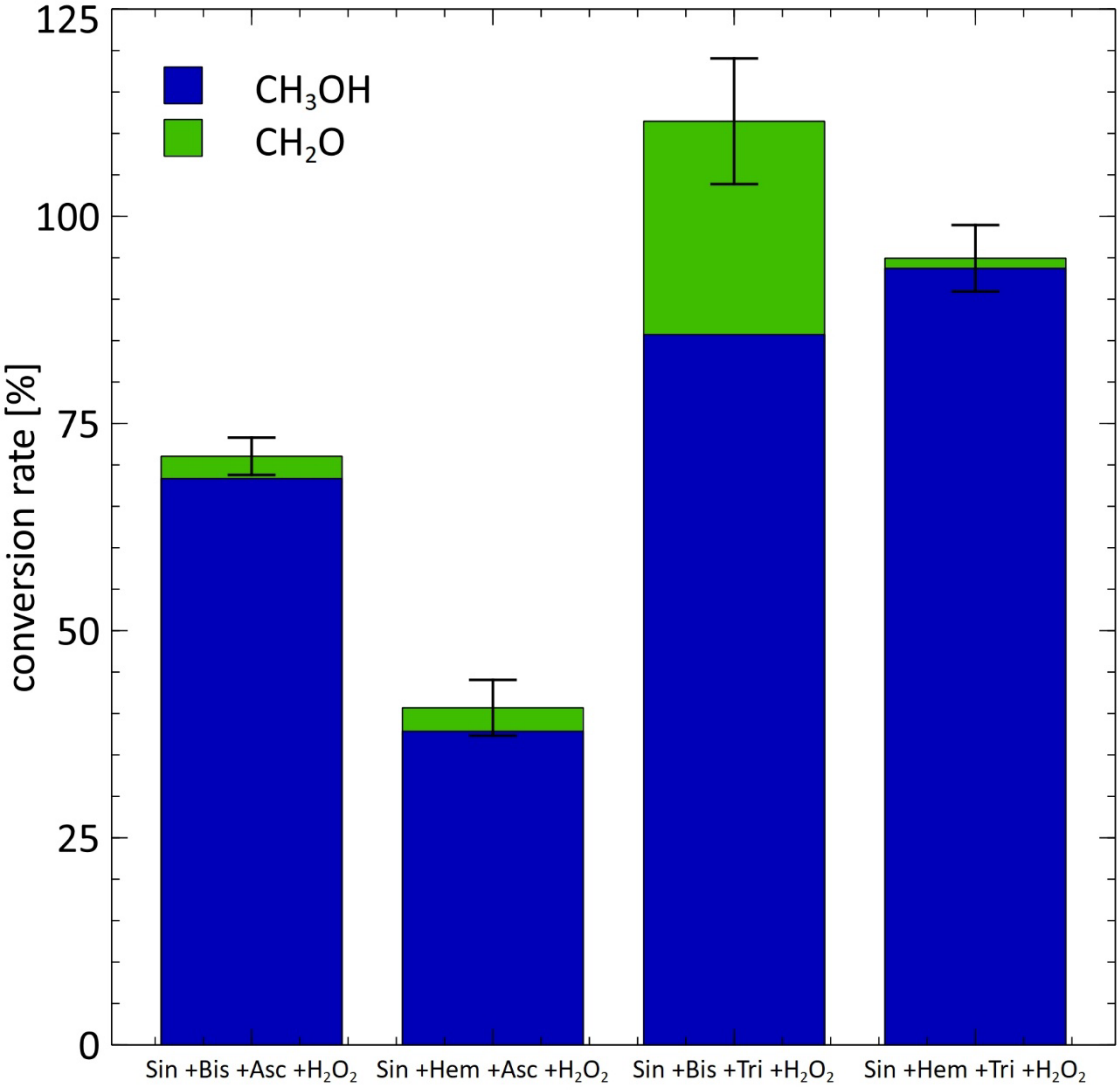

Fig. S3: Conversion rates of sinapyl alcohol to CH_3OH and CH_2O with $[(L)Fe^{II}Cl_2]$ or Fe_2O_3, triflic acid or ascorbic acid, and H_2O_2

Formation of CH_3OH and CH_2O from sinapyl alcohol in experiments mediated 10 µmol $[(L)Fe^{II}Cl_2]$, or Fe_2O_3 with 200 µmol H_2O_2, and 0.05 µmol triflic acid or 100 µmol ascorbic acid. Reactions were performed in 10 mL H_2O. All provided data were evaluated at 22 °C and ambient pressure (1013 mbar) after 48 h reaction time. Conversion rates were related to one methoxy group. Error bars represent the standard deviation (SD) of total CH_3OH and CH_2O conversion, based on the mean of three independent experiments (n=3), each measured in triplicate.

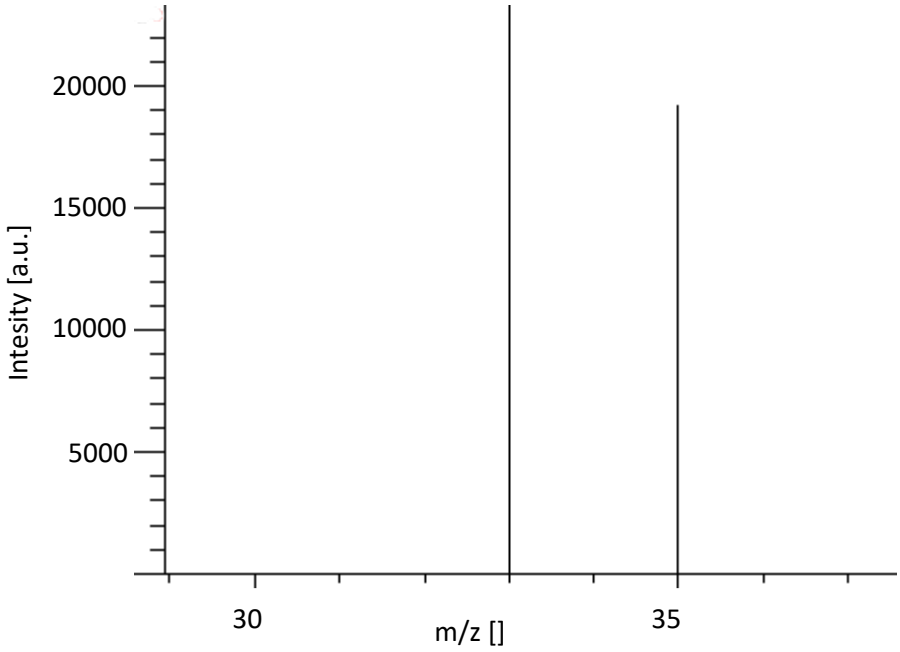

Fig. S4: Mass track of CH_3OH in standard experiments with d_3-2-methoxyphenol

The mass tracking of labeled CH_3OH from experiments involving d_3-2-methoxyphenol was measured in the headspace. This comprised using 25 µmol of d_3-2-methoxyphenol, along with 200 µmol of H_2O_2, 10 µmol of $[(L)Fe^{II}Cl_2]$, and 0.05 µmol of triflic acid (at pH=2.3), all dissolved in 10 mL of H_2O. Characteristic masses of 33 and 35 were observed for the labeled CH_3OH. The detection of mass 35 indicates that all three deuterium (^2H) atoms from the d_3-2-methoxyphenol are present in the labeled CH_3OH.

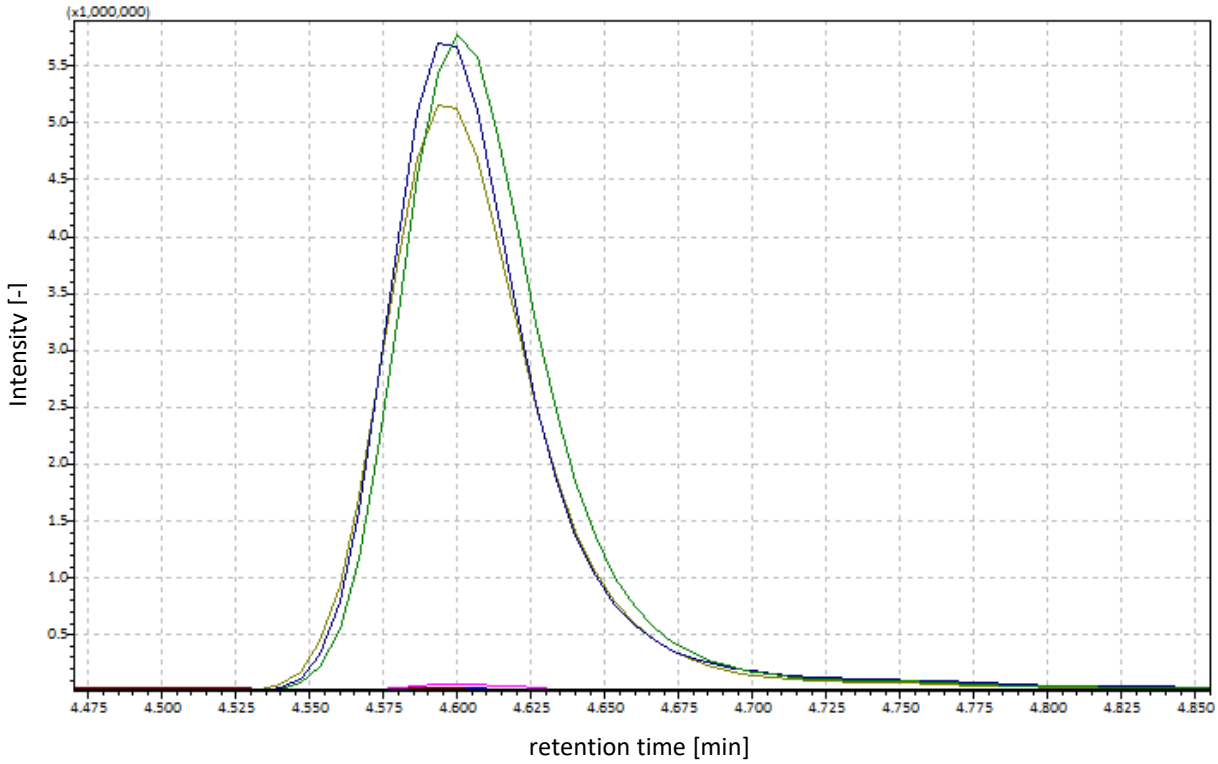

Fig. S5: Measurements of CH_3OH in standard experiments with $^{18}OCH_3$-2-methoxyphenol

Experiment with 2 µmol $^{18}OCH_3$ 2-methoxyphenol, 20 µmol H_2O_2, 1 µmol $[(L)Fe^{II}Cl_2]$, and 0.005 µmol triflic acid (pH=2.3) dissolved in 1 mL H_2O. Pink, blue, and brown chromatograms are the measured mass of 29, 30, and 31 of the produced CH_3OH (small to no peaks) in experiments with $^{18}OCH_3$ 2-methoxyphenol. The black line is the blank without substrate (no peak), and green, dark blue, and olive are the masses 33 and 34 of CH_3OH (large peaks) measured in the same experiments.

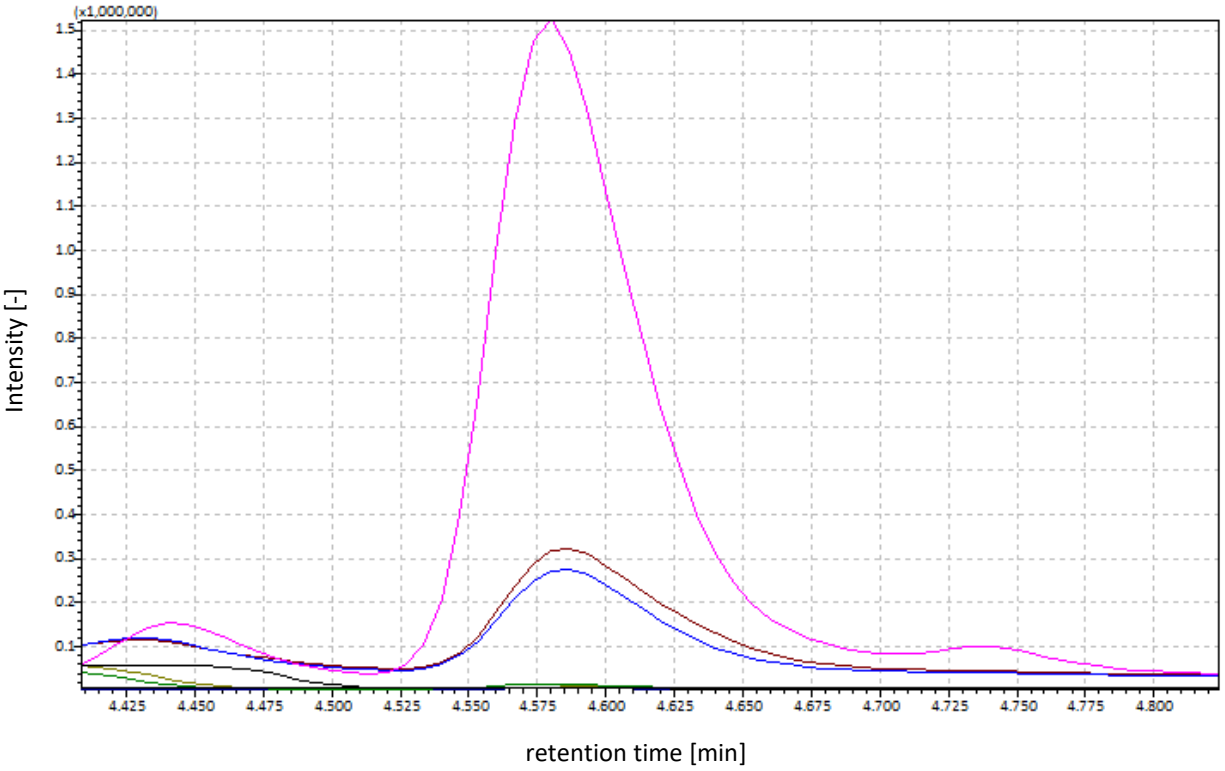

Fig. S6: Measurements of CH_3OH in standard experiments with $H_2{}^{18}O_2$ instead of H_2O_2 in the headspace and in H_2O.

Experiment with 25µmol substrate (sinapyl alcohol, coniferyl alcohol, or 2-methoxyphenol), 200µmol $H_2{}^{18}O_2$, 10 µmol $[(L)Fe^{II}Cl_2]$, and 0.05 µmol triflic acid (pH=2.3) dissolved in 10 mL H_2O. Pink, blue, and brown chromatograms are the measured mass of 29,30, and 31 of the produced CH_3OH (large peaks) in experiments with sinapyl alcohol, coniferyl alcohol, and guaiacol. The black line is the blank without substrate (no peak), and green, dark blue, and olive are the masses 33 and 34 of CH_3OH measured in the same experiments (small to no peaks).

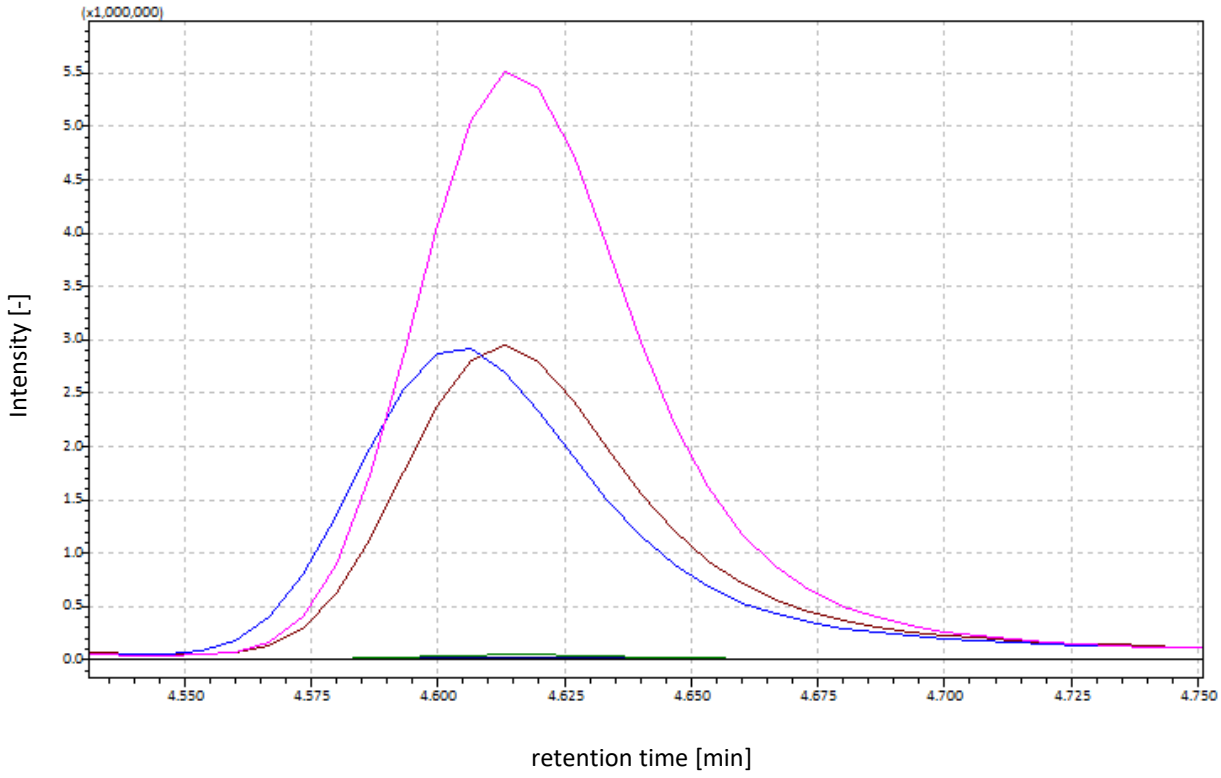

Fig. S7: Measurements of CH_3OH in standard experiments with $^{18}O_2$ instead of atmospheric O_2 in the headspace and in H_2O.

Experiment with 25µmol substrate (sinapyl alcohol, coniferyl alcohol, or 2-methoxyphenol), 200µmol H_2O_2, 10 µmol $[(L)Fe^{II}Cl_2]$, and 0.05 µmol triflic acid (pH=2.3) dissolved in 10 mL H_2O. Pink, blue, and brown chromatograms are the measured mass of 29,30, and 31 of the produced CH_3OH (large peaks) in experiments with sinapyl alcohol, coniferyl alcohol, and guaiacol. The black line is the blank without substrate (no peak), and green, dark blue, and olive are the masses 33 and 34 of CH_3OH (small to no peaks) measured in the same experiments.

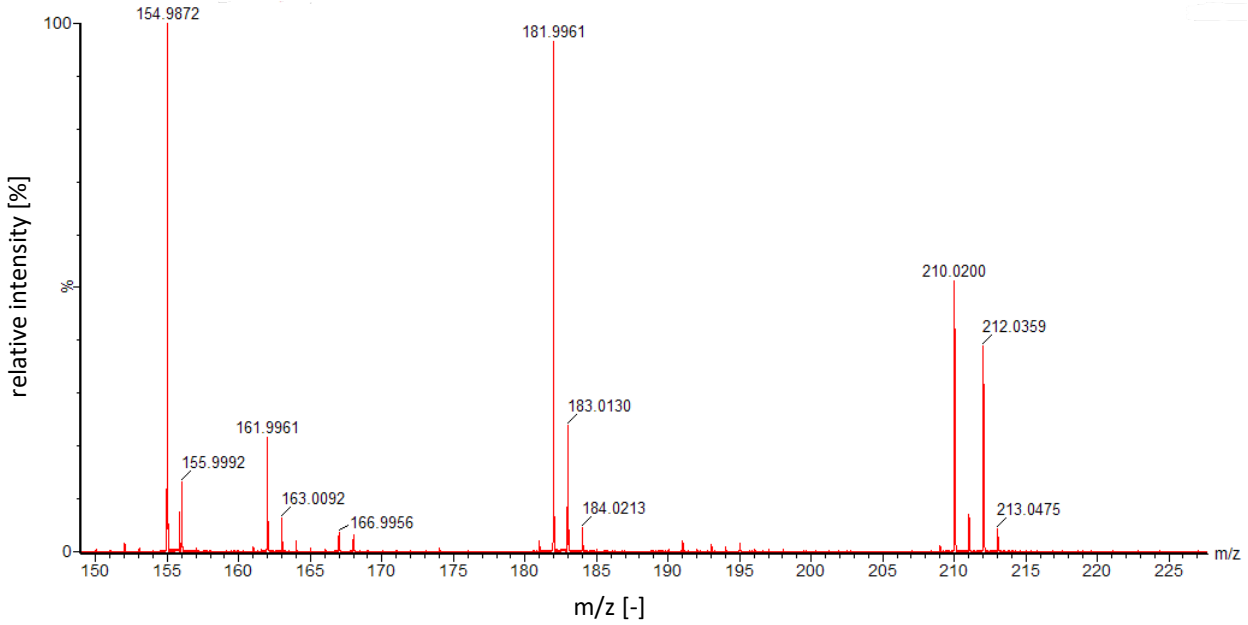

Fig. S8: Mass track of CH_2O in standard experiments with d_3-2-methoxyphenol

The mass tracking of labeled CH_2O from experiments with d3-2-methoxyphenol was conducted using a standard protocol. This involved utilizing 25 µmol of d_3-2-methoxyphenol, along with 200 µmol of H_2O_2, 10 µmol of $[(L)Fe^{II}Cl_2]$, and 0.05 µmol of triflic acid (at pH=2.3), all dissolved in 10 mL of H_2O. Characteristic masses of 155, 182, and 210 were observed for the derivatized CH_2O. Additionally, the mass of 212 was identified for the CD_2O, which originated from d3-2-methoxyphenol.

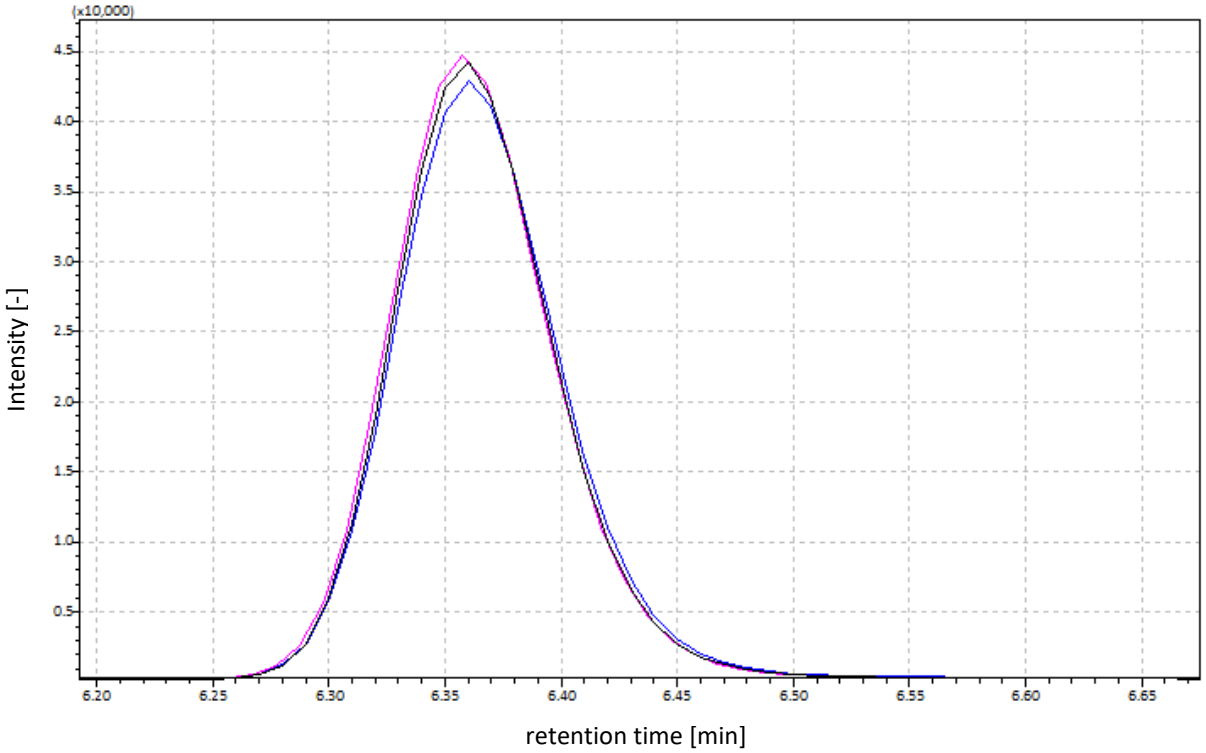

Fig. S9: Chromatogram of CH_3Br in alkyl radical trapping experiments with CCl_3Br as a scavenger

Measurement of mass 94 (stable isotope 79 of bromine) and mass 96 (stable isotope 81 of bromine) in experiments with sinapyl alcohol (pink) or 2-methoxyphenol (blue) (25 µmol substrate, 200 µmol of H_2O_2, 10 µmol of $[(L)Fe^{II}Cl_2]$, and 0.05 µmol of triflic acid (at pH=2.3), all dissolved in 10 mL of H_2O). The black line is the blank without a substrate. No differences were measured between blank experiments and experiments with sinapyl alcohol and 2-methoxyphenol.

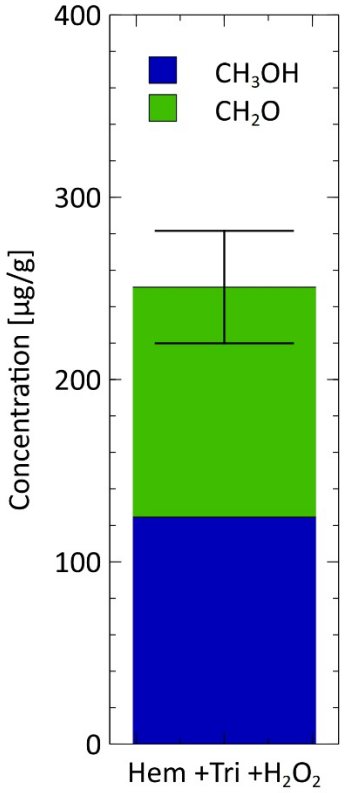

Fig. S10: Conversion rates of lignin to CH_3OH and CH_2O with Fe_2O_3, triflic acid and H_2O_2

Formation of CH_3OH and CH_2O from Lignin in experiments mediated 10 µmol Fe_2O_3 with 200 µmol H_2O_2, and 0.05 µmol triflic acid. Reactions were performed in 10 mL H_2O. All provided data were evaluated at 22 °C and ambient pressure (1013 mbar) after 48 h reaction time. Conversion rates were related to one methoxy group. Error bars represent the standard deviation of total CH_3OH and CH_2O conversion, based on the mean of three independent experiments (n=3), each measured in triplicate.

Table S2: Soil samples from this study and reference[1]. TOC and methoxy content in w%. pH value was directly measured in the experiment after 48 h of incubation. Total iron content measured in [w%].

Soil sample	TOC [w%]	Methoxy content [w%]	pH	Total iron content [%]
Birkenheide 10-25 cm	0.14	0.012	4.71	0,16
Birkenheide 25-35 cm	-0.13	0.005	5.70	0,15
Malchenberg 5-15 cm	2.12	0.065	7.24	0,40
Walldorf 20-35 cm	-0.58	0.009	5.22	0,37
Walldorf 5-15 cm	1.23	0.036	4.21	0,36
Walldorf Oberboden	3.55	0.129	4.14	0,97
Schriesheim 1 0-5 cm	3.75	0.076	3.62	1,74
Schriesheim 2 Oberboden	1.06	0.033	7.47	1,85
Schriesheim 2 45-55 cm	0.93	0.023	7.63	0,27
Maxdorf Oberboden	4.35	0.123	3.87	0,26
Maxdorf 5-15 cm	4.08	0.143	3.96	0,24
Maxdorf 15-30 cm	-0.61	0.011	5.30	1,58
Altlußheim ~20 cm	11.2	0.188	7.11	4,13
Hockenheim ~25 cm	6.19	0.197	7.60	3,37
Hockenheim 10-20 cm (GL1)	7.83	0.170	7.42	2,64
Walldorf SAP Wald 40-90 cm	0.07	0.004	5.20	0,56
Walldorf SAP Wald 10-40 cm	0.79	0.023	4.00	0,44
Walldorf SAP Wald 0-10 cm	16.2	0.423	3.50	0,40
Peterstal Berg Wald 10-40 cm	2.15	0.030	3.70	0,94
Peterstal Berg Wald 0-10 cm (PO)	8.07	0.139	3.20	0,75
Unterhof Wald 20-100 cm	0.59	0.014	7.90	2,80
Unterhof Wald 0-10 cm (CH)	3.63	0.103	7.4	1,75
ST. Leon-Rot 10-40 cm	5.64	0.052	7.6	2,47
ST. Leon-Rot 0-10 cm	2.80	0,085	7.8	2,28

Detailed TOC–methoxy–C_1 correlations

In these soils and additionally the previously studied soils, the methoxy group content and the TOC were measured (Fig. S11a)[1]. A high correlation between TOC and methoxy content (R^2 = 0.88) was observed, indicating that a significant proportion of TOC is lignin-derived due to its high methoxy content. Additionally, the high correlation of the TOC with the produced CH_3OH and CH_2O (Fig. S11b) indicates that the TOC measurement gives a good prediction for the CH_3OH and CH_2O production of the soil and also that the production decreases with depth due to the normally decreasing TOC (Fig. S11b). Also, a correlation (R^2) of 0.60 is displayed in Fig. S11c of the methoxy content with the produced CH_3OH and CH_2O

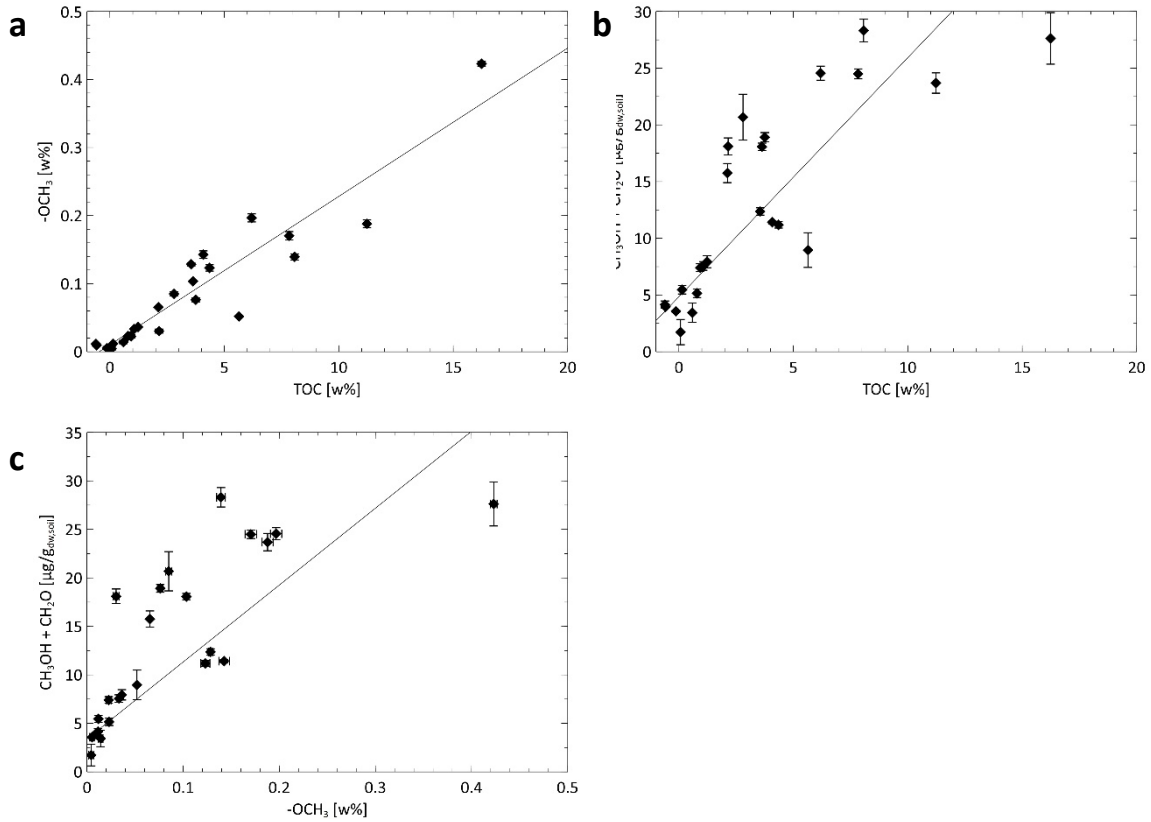

Fig. S11: Correlations between soil TOC and methoxy content, as well as between TOC or methoxy content with CH_3OH + CH_2O production in sterile soils.

a) Correlation of the TOC (n = 1) with OCH_3 content (n = 3) of the investigated soil samples and additionally those previously investigated[1] with an R^2 = 0.88. **b)** Correlation of the TOC with the sum of CH_3OH and CH_2O concentrations (R^2 = 0.67) in the identical soil samples. **c)** Correlation of the OCH_3 content with the sum of CH_3OH and CH_2O concentrations (R^2 = 0.60) in the identical soil samples. The experiments involved a two-day incubation period, during which 5 g of sterile soil was incubated in 10 ml ultra-pure H_2O.

Zeisel method application and removal of the methoxy content of three soils

Additional insight into the role of methoxy groups in abiotic C1 compound formation were gained through soil experiments involving chemical demethoxylation using the Zeisel method[2], which employs hydroiodic acid to cleave methoxy groups from lignin. Following this treatment (Fig. S12a), the methoxy content in three selected soils (GL1, PO, and GL2) was reduced by 81.1% to 93.6%. As a result, CH_3OH production was completely abolished in all treated samples (Fig. S12b), while CH_2O concentrations were reduced by up to 83.5%. The residual

CH_2O detected may stem from incomplete removal of methoxy groups. However, alternative explanations cannot be excluded: (i) the absence of CH_3OH may result from its rapid oxidation to CH_2O due to sufficient oxidative capacity in the soil system, and (ii) a portion of the CH_2O may originate from non-methoxy carbon precursors, as suggested by earlier model compound experiments involving aromatic substrates lacking methoxy groups[1]. Nonetheless, the complete suppression of CH_3OH formation and the substantial reduction in CH_2O levels in demethoxylated soils provide strong evidence that both compounds primarily derive from native methoxy groups in soil organic matter.

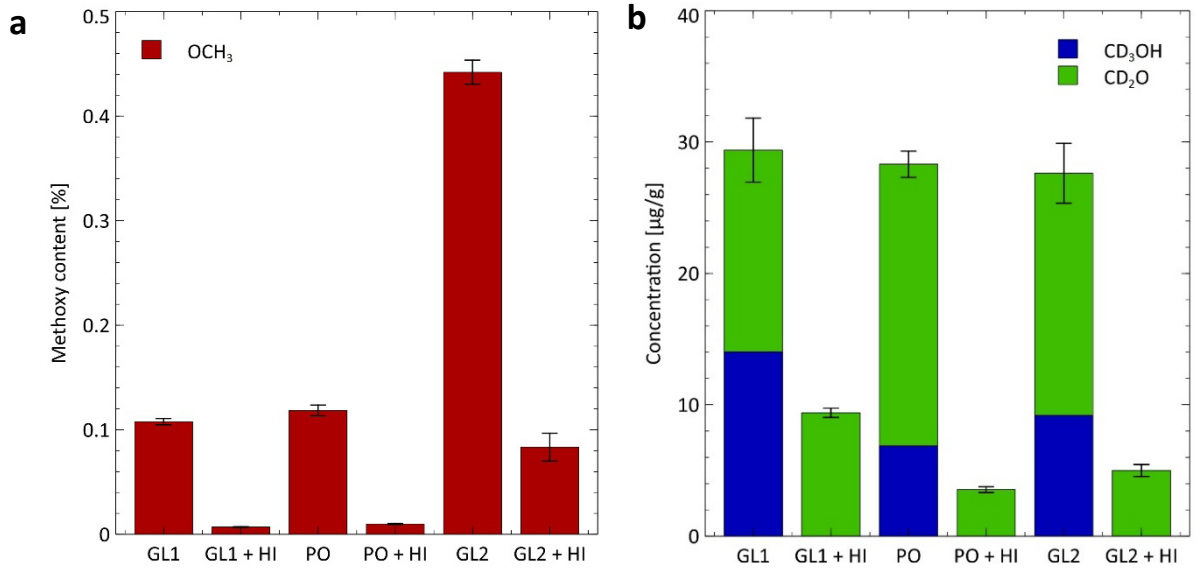

Fig. S12: Soil methoxy content and formation of CH_3OH and CH_2O from soils before and after chemical removal of methoxy groups. a) Methoxy group content in soils (30 g) GL1 (0–20 cm), PO (0–10 cm), and GL2 (0–10 cm) before and after treatment with hydroiodic acid (HI, 25 ml; 57 % at 105 °C for 2 h). **b**) Formation of CH_3OH and CH_2O in the same soils (5g in 10 ml ultrapure water at 22 °C and 1013 mbar) before and after chemical removal of methoxy groups. Error bars represent the standard deviation from $n = 3$ independent measurements for methoxy content **(*a*)** and of the total CH_3OH and CH_2O conversion, based on the mean of three independent experiments (n = 3), each measured in triplicate **(*b*)**.

Isotopic labeling experiments in HI-treated soils

To unequivocally confirm that hydroiodic acid–treated soil (GL+HI) retains the ability to convert externally supplied methoxy groups into CH_3OH, we conducted isotopic labeling experiments. Isotopically labelled 2-methoxyphenol—either with a fully deuterated methyl group (d_3) or with an ^{18}O-labelled methoxy oxygen—was added to aqueous suspensions of the HI-treated soil. The formation of CH_3OH containing either the ^{18}O label or all three deuterium atoms was successfully detected (Fig. S13 a, b). These results clearly demonstrate that the demethoxylated soil system remains reactive and can transform 2-methoxyphenol into CH_3OH via the same mechanism observed in the model compound experiments. This supports the idea that native soil conditions—characterized by abundant lignin-derived methoxy groups, iron-bearing minerals, and continuous in situ production of reactive oxygen species (e.g., H_2O_2 and •OH)[3–6]—can drive abiotic CH_3OH formation.

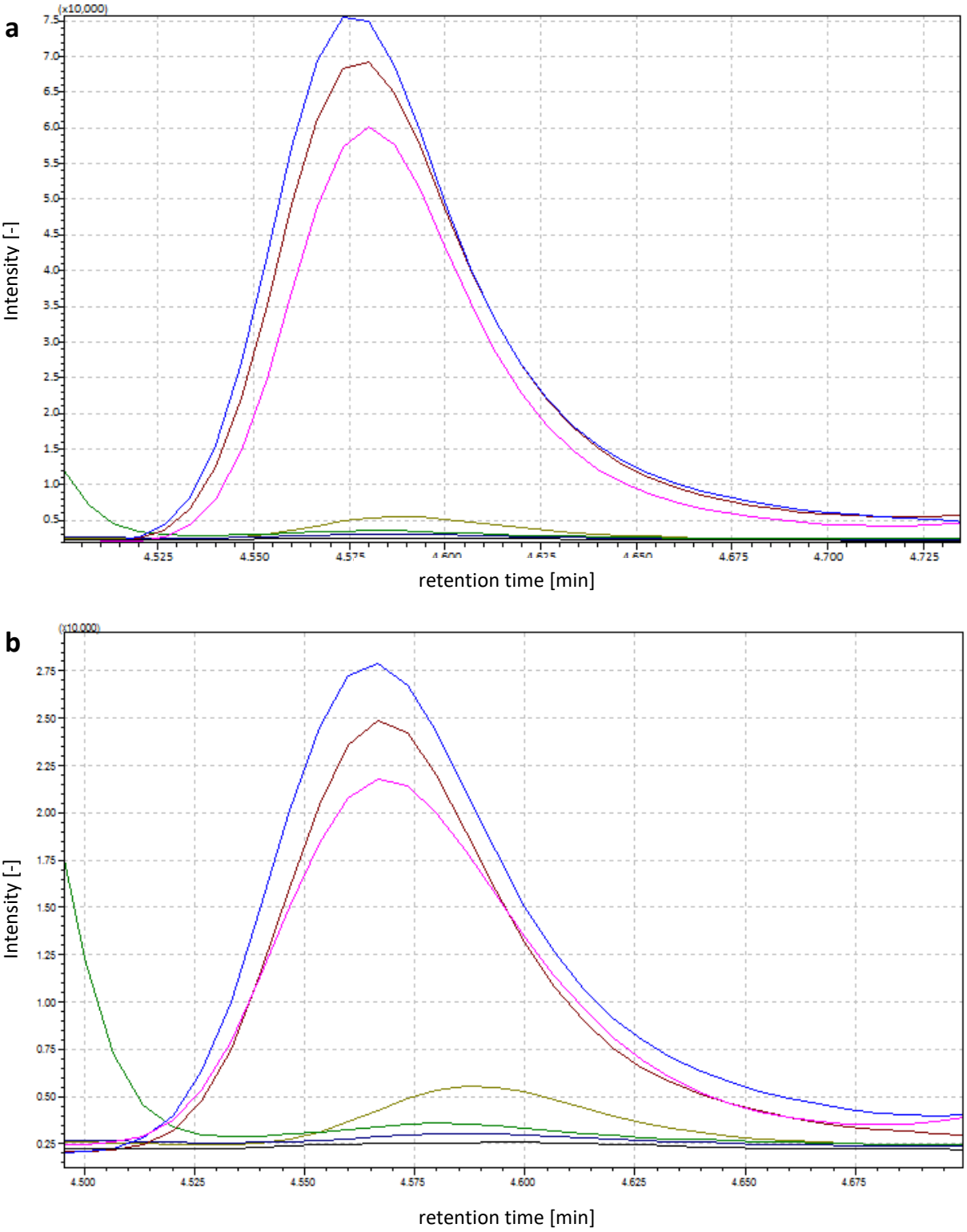

Fig. S13: Chromatogram of labeled CH_3OH in soil experiments with added ^{2}H and ^{18}O labelled 2-methoxyphenol

Chromatogram of mass 33,34 and 35 of $C^{2}H_3OH$ **(a)** or mass 33 and 34 of $CH_3{}^{18}OH$ **(b)** in experiments were the methoxy groups were removed from the soil samples GL1, PO and GL2 using the Zeisel method [2] with 1 g soil and 2 ml H_2O with added 5µmol **(a)** d3-2-methoxyphenol and **(b)** 5 µmol ^{18}O-2-methoxyphenol. Blue, brown, and pink are the experiments with labelled

2-methoxyphenol (large peaks), light green, dark green, and purple are the non-spiked soils (small to no peaks), and black (no peak) is pure H_2O. A production of labeled CH_3OH is clearly visible compared to the unlabeled soils and pure H_2O.

pH manipulation experiments with soil PO

The investigated soil samples spanned a pH range of 3.50 to 7.63, representing typically acidic soils widely distributed across terrestrial ecosystems. To assess the influence of pH on abiotic C_1 compound formation, we selected soil sample PO, which had an initial pH of 3.2, and incrementally adjusted it to more neutral values (pH 3.9, 5.2, 6.2, and 6.9). As shown in Fig. S14, CH_3OH concentrations increased consistently with rising pH. In contrast, CH_2O concentrations generally declined with increasing pH, except for a slight increase observed at pH 6.9. The total yield of CH_3OH and CH_2O remained relatively constant across treatments, within the margin of experimental error, apart from a modest elevation at pH 6.9. These patterns may be explained by the pH-dependent redox behavior of iron: at higher pH, Fe^{3+} is increasingly reduced to Fe^{2+},[7] which then requires additional oxidative capacity (e.g., H_2O_2 or ROS) to regenerate reactive Fe^{4+}=O species. Also, the Fe^{3+} has, in general, a much lower solubility than Fe^{2+}.[7] This shift may reduce the availability of oxidants required to convert CH_3OH to CH_2O, thereby promoting CH_3OH accumulation at higher pH levels. Moreover, it is difficult to directly compare the soil experiments with model studies in homogeneous solution.

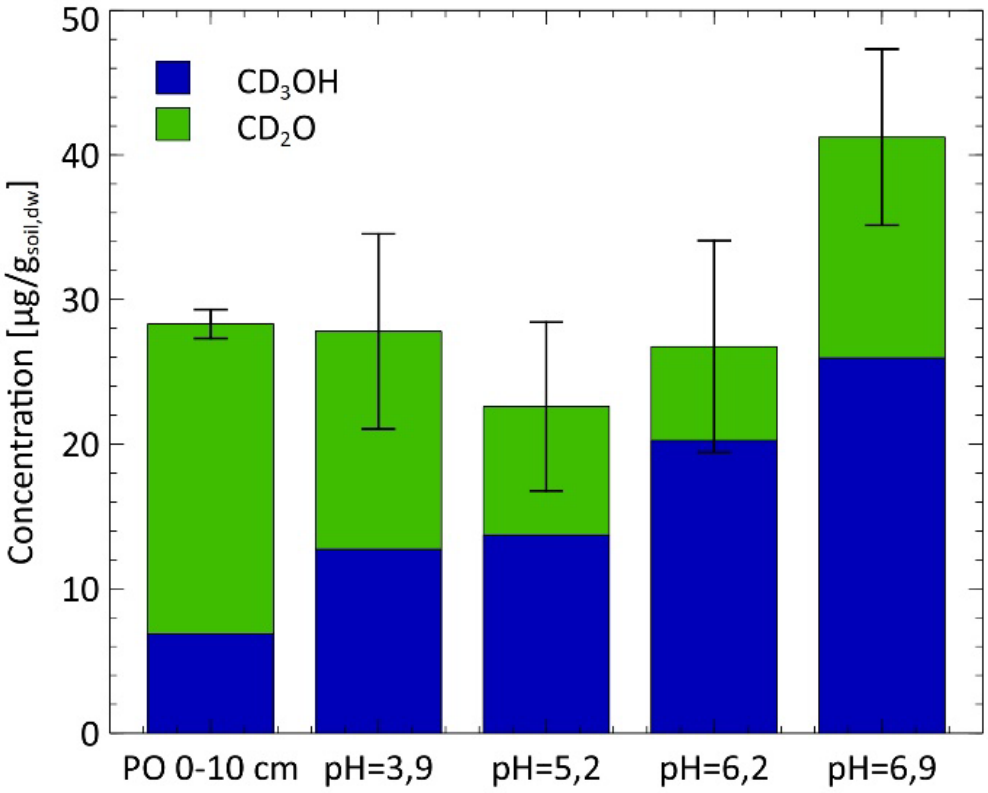

Fig. S14: Abiotic formation of CH_3OH and CH_2O in soil experiments at different pH-values

Formation of CH_3OH and CH_2O from soil sample PO 0-10 incubated under sterile aqueous conditions with pH adjustments with NaOH (3.2-6.9). Soils (5 g each) were suspended in ultrapure water (10 mL) and incubated for 48 hours at ambient temperature and pressure (22 °C, 1013 mbar). Error bars represent the standard deviation of total CH_3OH and CH_2O conversion, based on the mean of three independent experiments (n=3), each measured in triplicate.

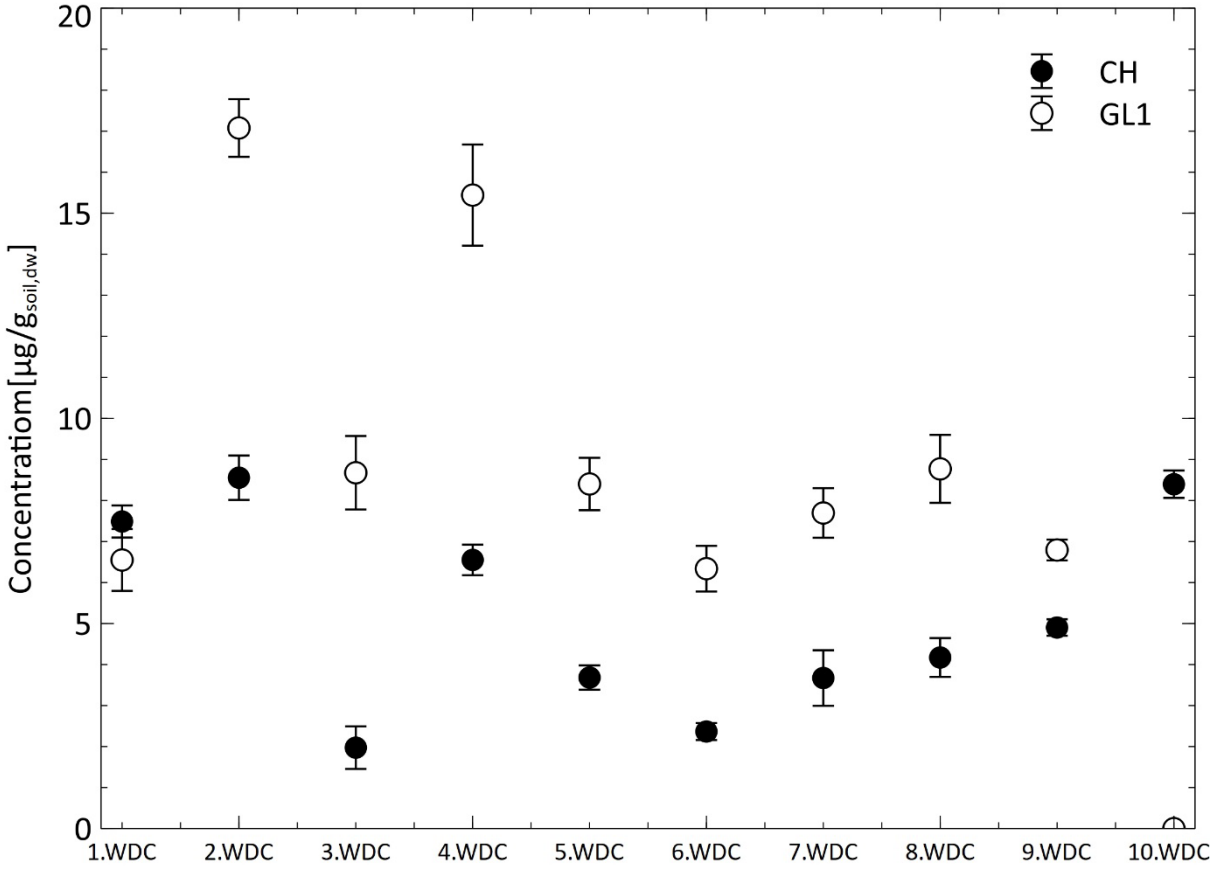

Fig. S15: CH_2O measurements in wet-dry-cycles with soil samples CH and GL1

Concentrations of CH_2O were measured across three wet-dry cycles of soil samples from CH and GL1. The reaction time was 48 h, followed by drying the soils at 105 °C for at least one day before rewetting them 10 times. The concentrations decreased from 7.49 ± 0.39 µg/$g_{soil, dw}$ and 6.55 ± 0.75 µg/$g_{soil, dw}$, to 4.90 ± 0.20 µg/g $_{soil, dw}$ and 6.79 ± 0.25 µg/g $_{soil, dw}$, respectively (at 10 WDC). CH_2O data from CH and GL1 could not be measured. This results in a total sum of 46.0 and 90.0 µg/$g_{soil,dw}$ of CH_2O. When converted to the total methoxy content in the soil, this represents a conversion of 4.44 and 4.79% of the methoxy groups to CH_3OH. Error bars represent the standard deviation of total CH_3OH and CH_2O conversion, based on the mean of three independent experiments (n=3), each measured in triplicate.

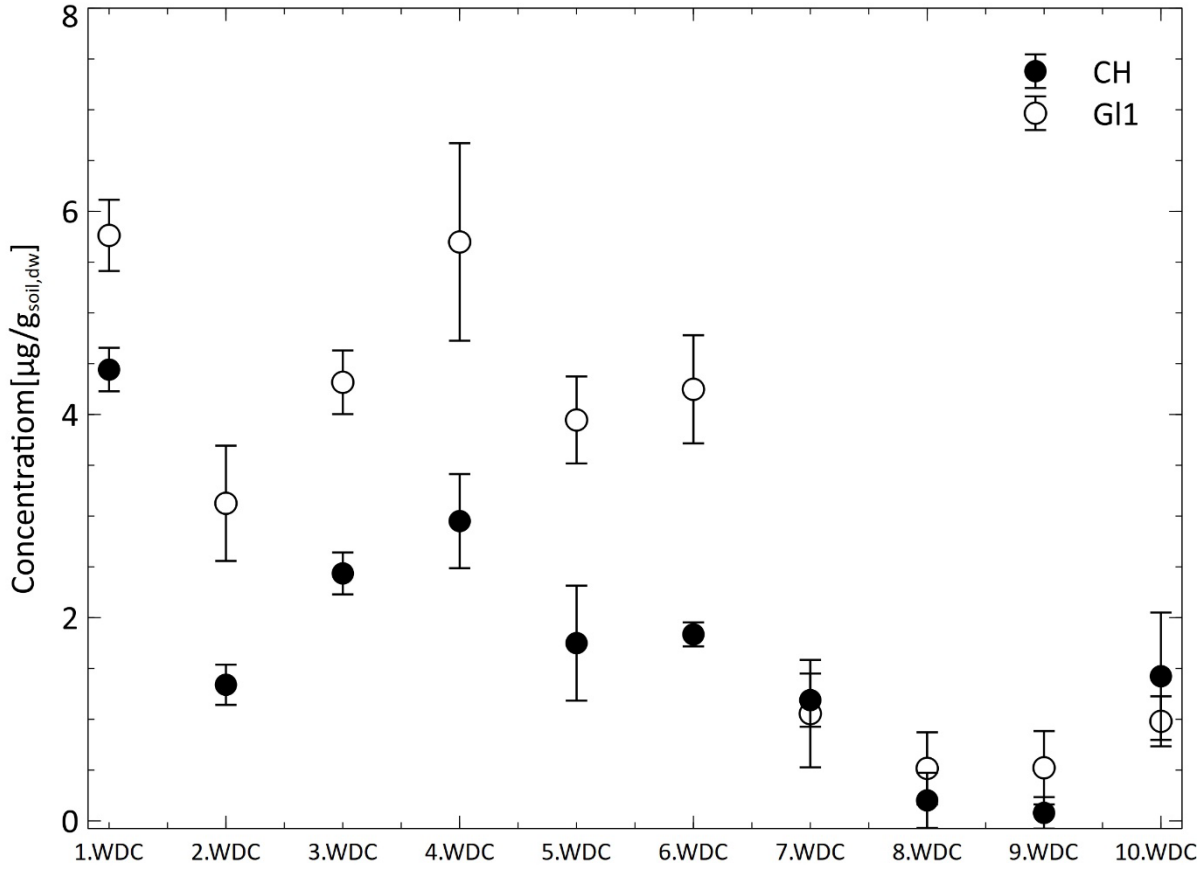

Fig. S16: CH_3OH measurements in wet-dry-cycles with soil samples CH and GL1

Concentrations of CH_3OH were measured across three wet-dry cycles of soil samples from CH and GL1. The reaction time was 48 h, followed by drying the soils at 105 °C for at least one day before rewetting and drying them 10 times. The starting concentrations are 4.44 ± 0.21 µg/$g_{soil,dw}$ and 5.76 ± 0.35 µg/$g_{soil,dw}$ and the final concentrations are 1.42 ± 0.63 µg/$g_{soil,dw}$ and 0.98 ± 0.25 µg/$g_{soil,dw}$, respectively. This results in a total sum of 18.1 and 31.6 µg/$g_{soil,dw}$ of CH_3OH. When converted to the total methoxy content in the soil, this represents a conversion of 1.74% and 1.68% of the methoxy groups to CH_3OH. Error bars represent the standard deviation of total CH_3OH and CH_2O conversion, based on the mean of three independent experiments (n=3), each measured in triplicate.

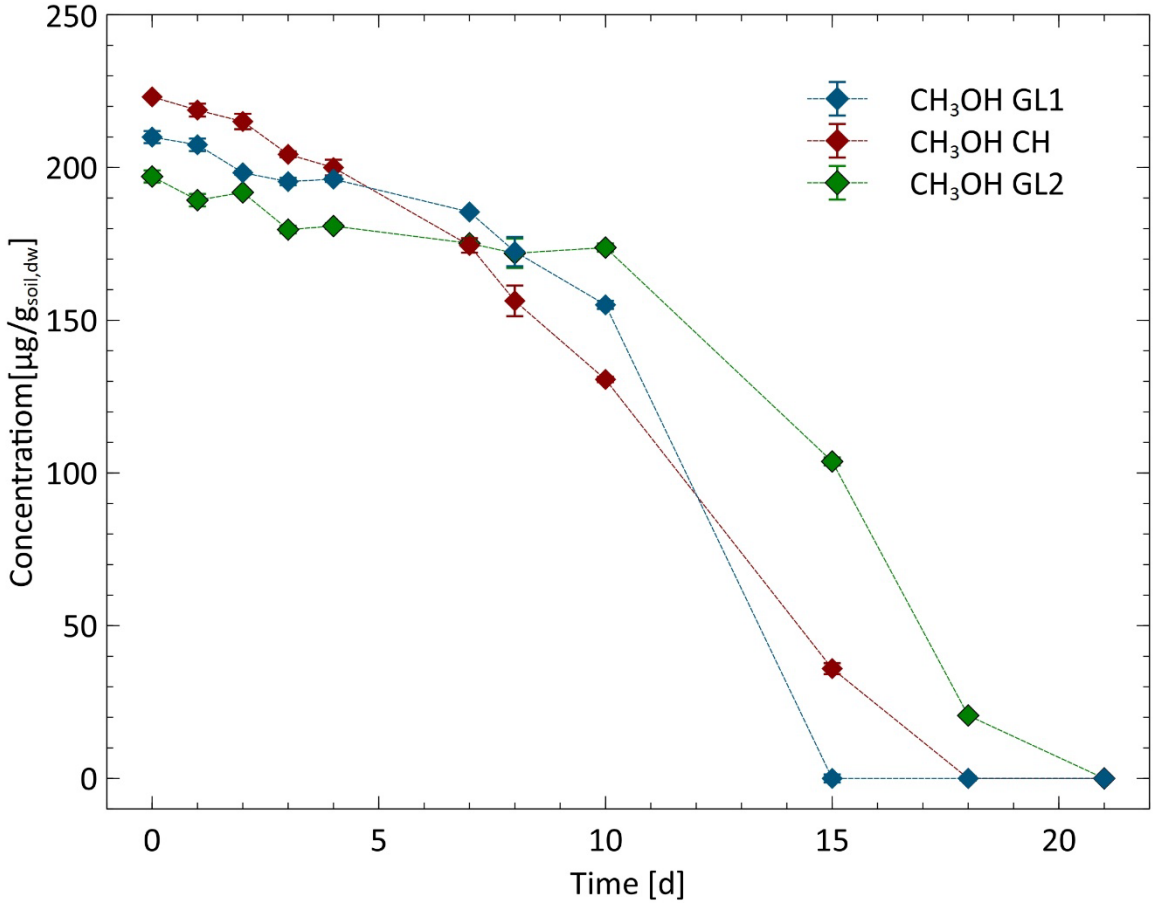

Fig. S17: Degradation of CH_3OH in fresh soils (GL1, CH, and GL2) due to microorganisms.

Concentrations of CH_3OH were measured over 21 days in one experiment for each soil (50 g) suspended in 100 mL ultra-pure H_2O and stored at 22 °C under ambient pressure (1013 mbar). The error bars represent the SD of the total conversion of CH_3OH in one experiment with triple measurements (n = 3).

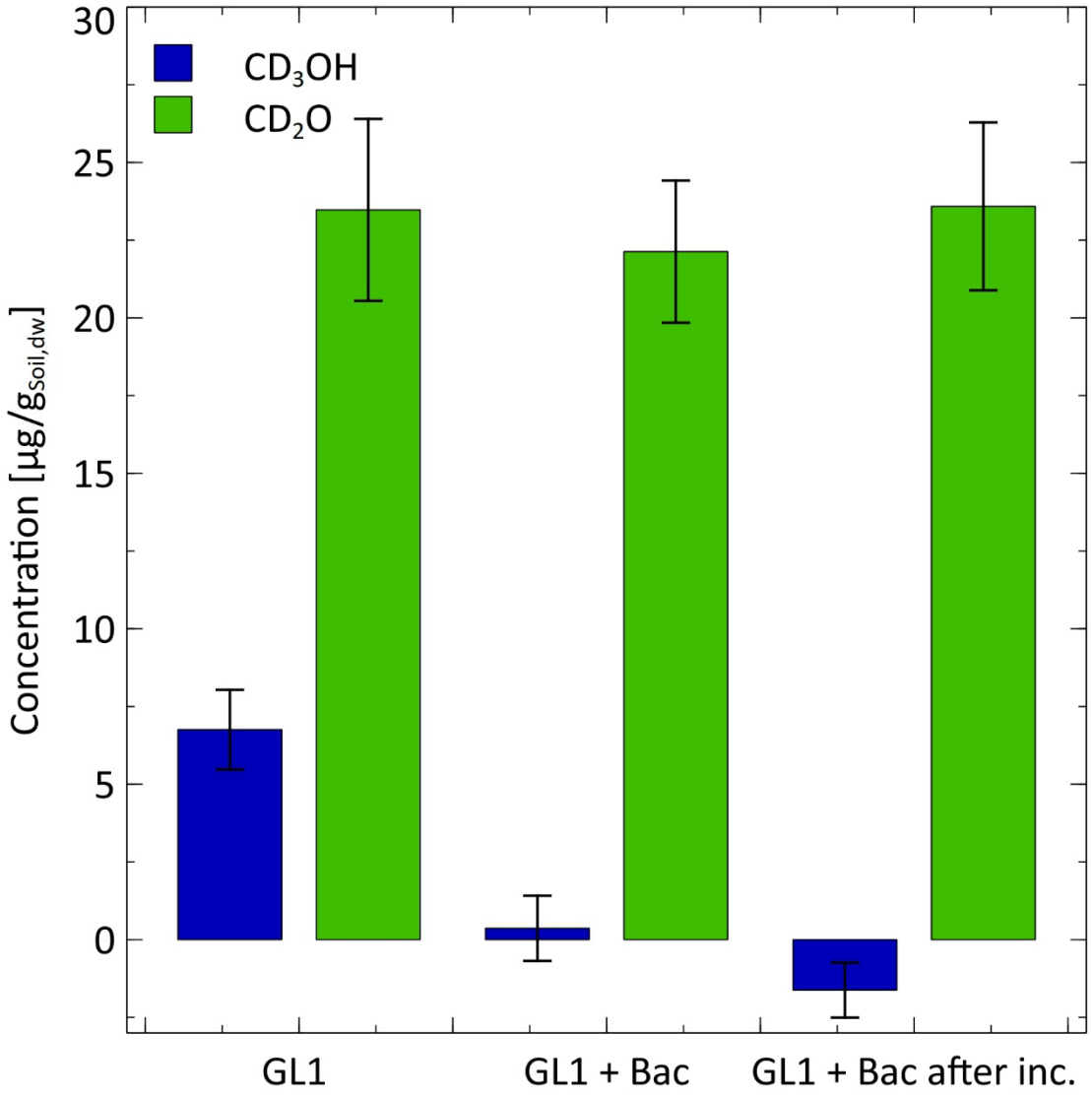

Fig. S18: Degradation of abiotic-produced CH_3OH in GL1 due to added methylotrophic bacteria

Addition of methylorubrum extorquens bacteria prior to and after the soil experiment GL1, with CH_3OH degradation in both experiments, and no changes in CH_2O concentration. CH_3OH and CH_2O measurements after 5 days in the experiment, when the bacteria were added after the abiotic experiment. Error bars represent the standard deviation (SD) of total CH_3OH and CH_2O conversion, based on the mean of three independent experiments (n=3), each measured in triplicate.

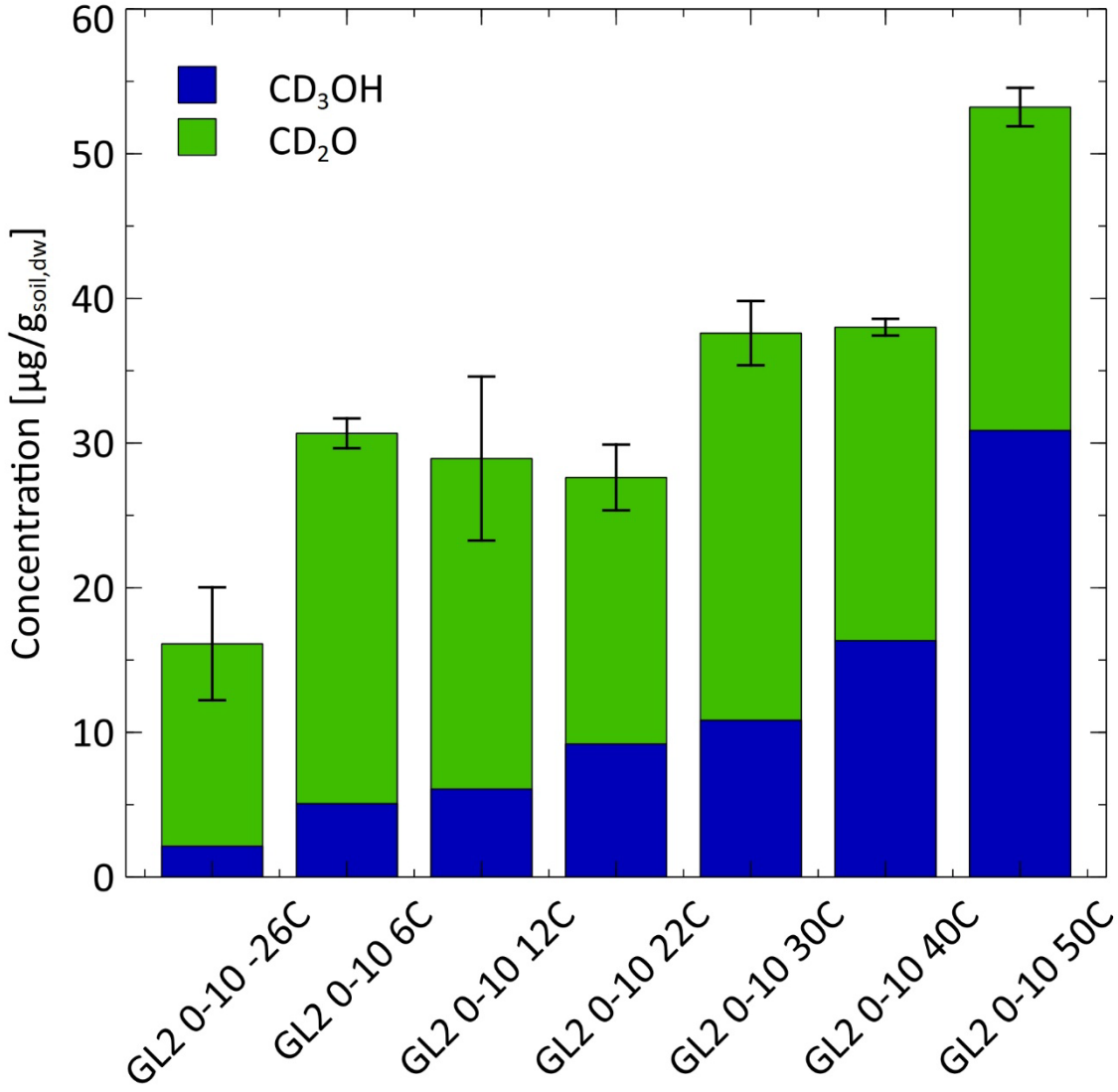

Fig. S19: Measurement of CH_3OH and CH_2O in soil GL2 as a function of temperature

Formation of CH_3OH and CH_2O from soil sample GL2 0-10 incubated under sterile aqueous conditions with different temperatures (-26 – 50 °C). Soils (5 g each) were suspended in ultrapure water (10 mL) and incubated for 48 hours under atmospheric pressure (1013 mbar). Error bars represent the standard deviation of total CH_3OH and CH_2O conversion, based on the mean of three independent experiments (n=3), each measured in triplicate.

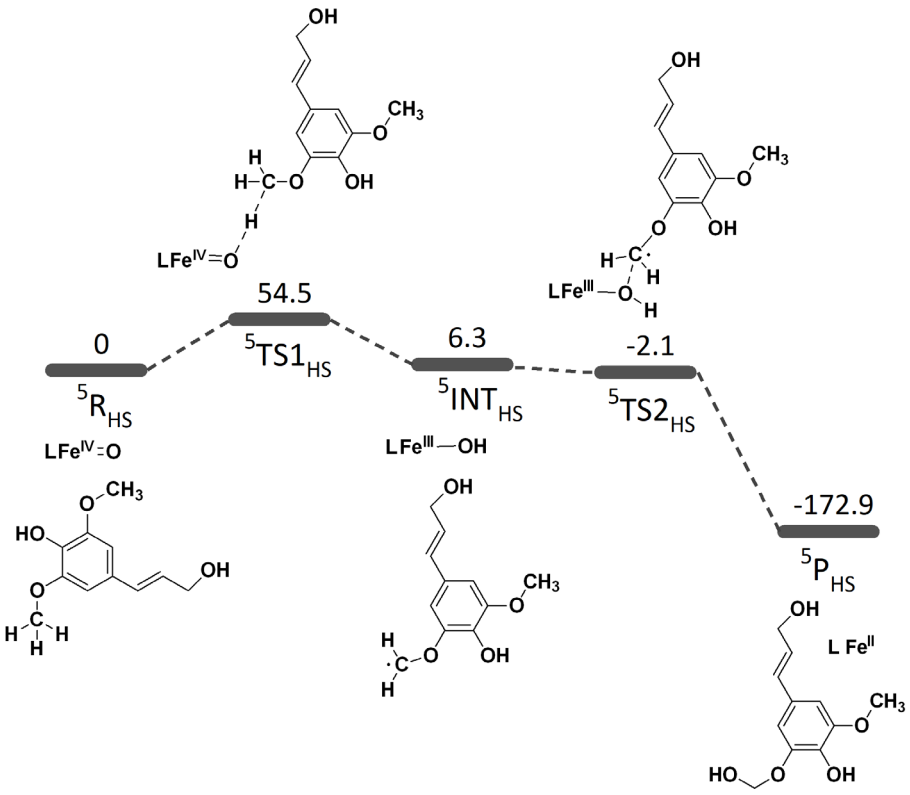

Fig. S20: Computed reaction profile of the HAA mechanism of sinapyl alcohol.

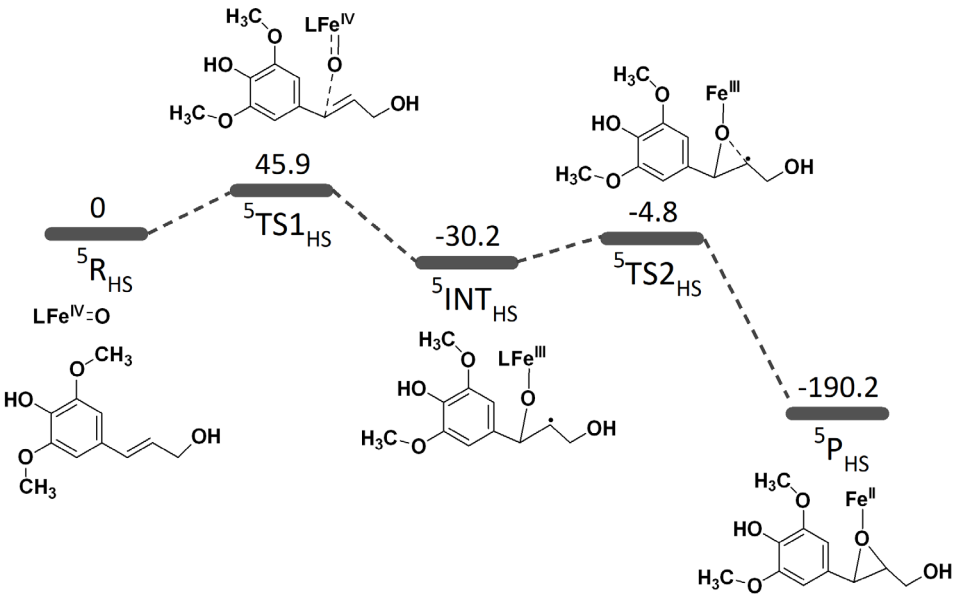

Fig. S21: Computed reaction profile of the OAT mechanism of sinapyl alcohol.

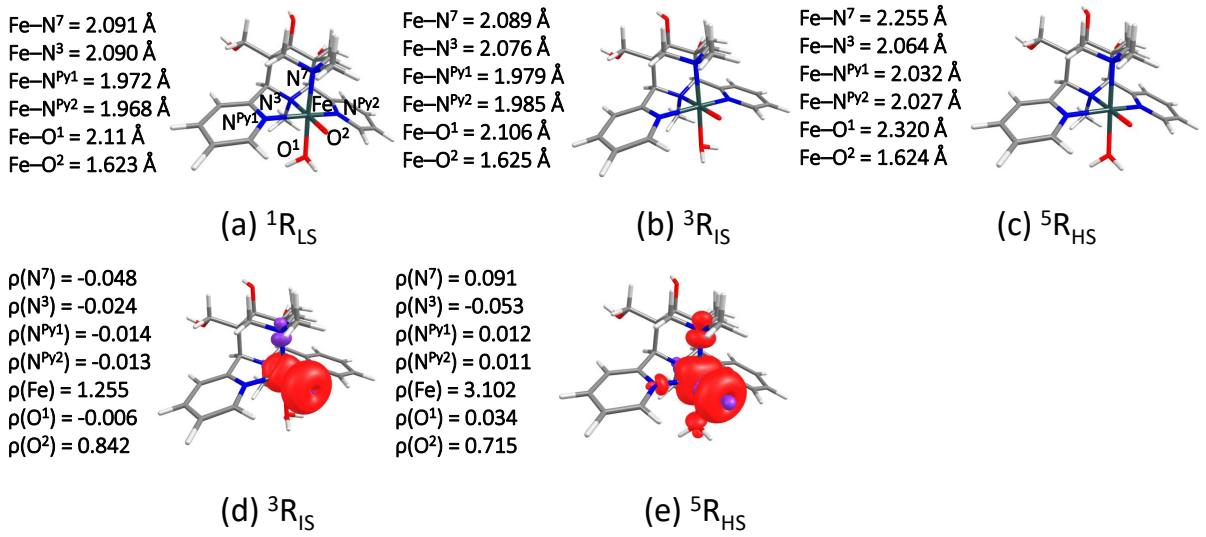

Fig. S22: Optimized geometries (a-c) and spin density plots (d-e) for $[(L)(OH_2)Fe^{IV}{=}O]^{2+}$.

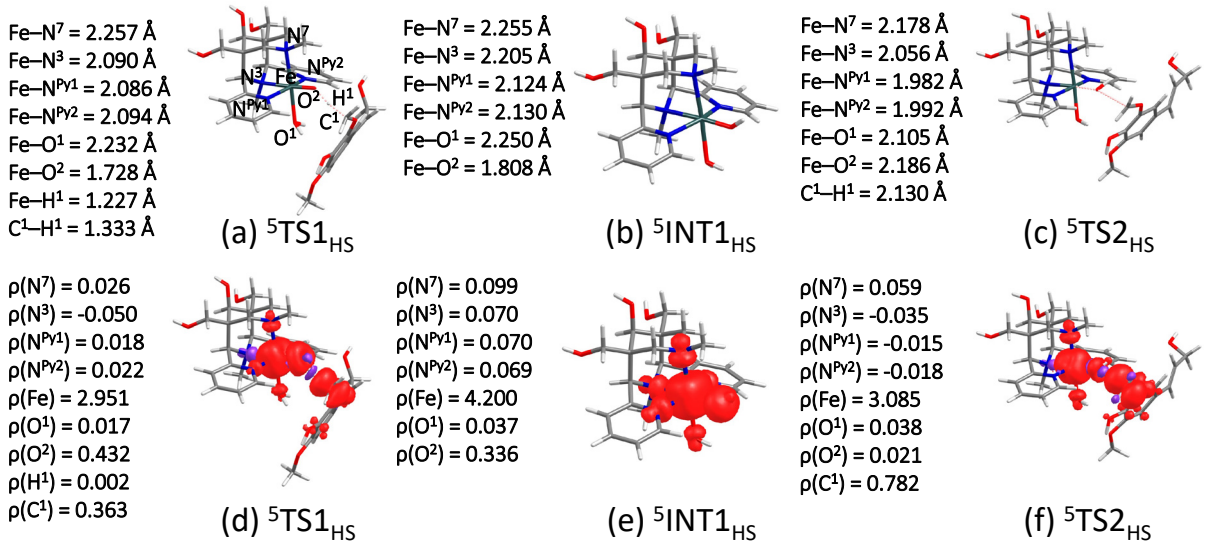

Fig. S23: Optimized geometries (a-c) and spin density plots (d-e) of HAA mechanism for $^5TS1_{HS}$, $^5INT1_{HS}$ and $^5TS2_{HS}$.

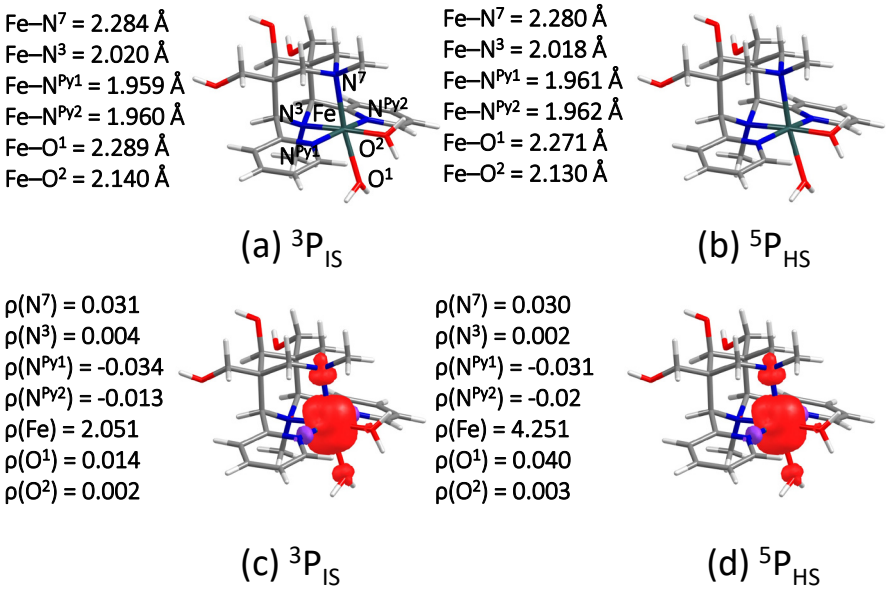

Fig. S24: Optimized geometries (a-c) and spin density plots (d-e) of HAA mechanism for $^{3}P_{IS}$, and $^{5}P_{HS}$.

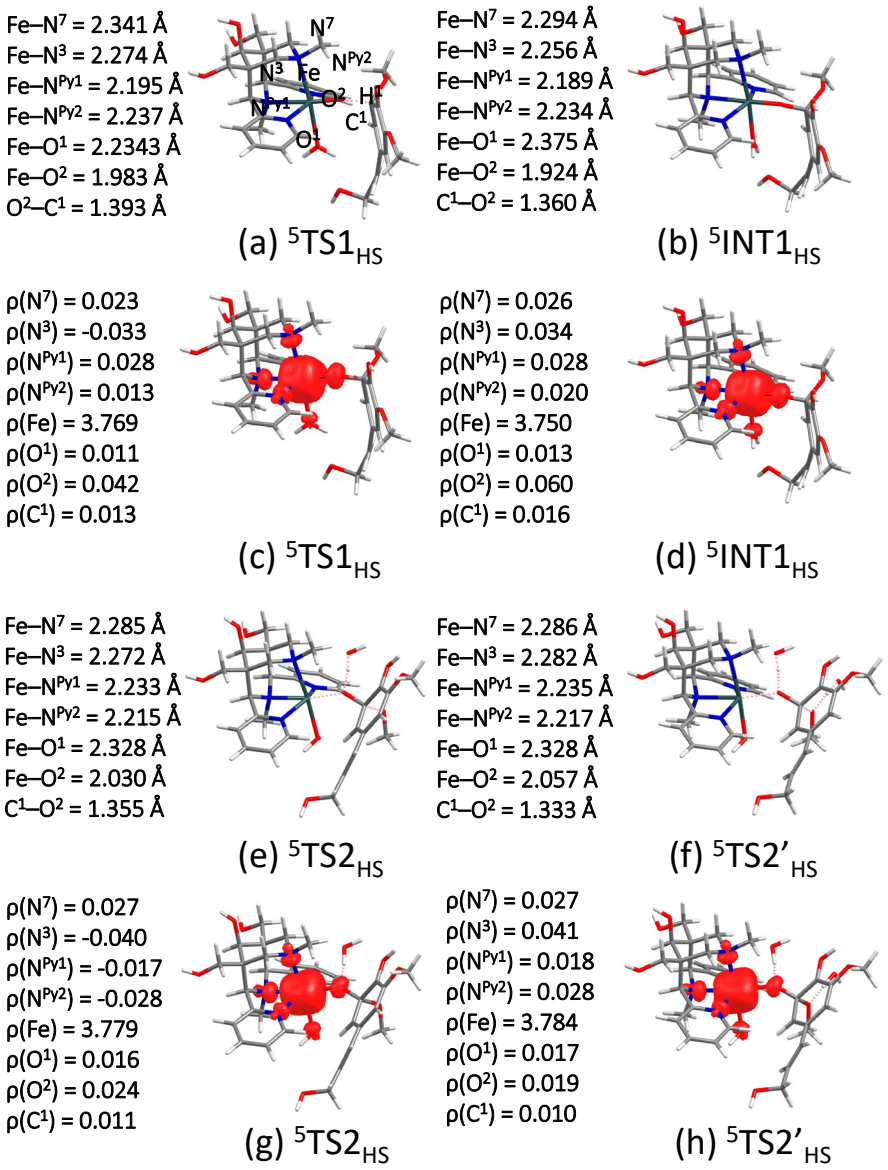

Fig. S25: Optimized geometries and spin density plots of demethoxylation mechanism for $^{3}TS1_{HS}$ (a, c), $^{3}INT1_{HS}$ (b, d), $^{3}TS2_{HS}$ (e, g) and $^{3}TS2'_{HS}$ (f, h).

To simulate an outer-sphere electron transfer mechanism, the formation of a substrate-catalyst complex, also involving HOtf molecules was examined. Initially, the Fe^{IV}-oxido center interacts with two HOtf molecules, forming an $[(L)Fe^{IV}{=}O(OH_2)...(HOtf)_2]$ precursor at -99kJ/mol. This reacts with a synapyl alcohol substrate molecule to the reactant complex (RC), which is highly stable with an energy of -139.5kJ/mol. Spin density values confirm that no electron transfer occurs during the formation of the reactant complex. In the subsequent step, the substrate approaches one of the HOtf molecules, where the close proximity to HOtf enables a PCET in a slightly endothermic step (+10.4kJ/mol). These findings suggest that both HAA and OAT reactions can occur via a PCET mechanism, with the HOtf molecule facilitating electron transfer through proton donation, indicating an outer-sphere electron transfer pathway (Figures S26-S28).

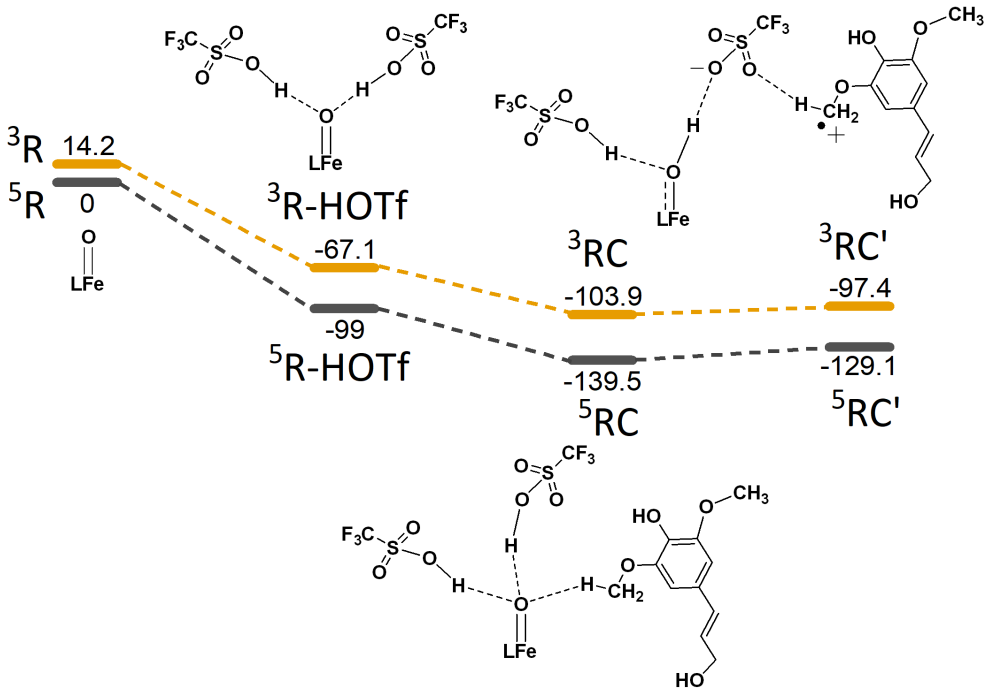

Fig. S26: Computed potential energy surface of $[(L)(OH_2)Fe^{IV}{=}O]^{2+}$ forming proton coupled electron transfer reactant complex.

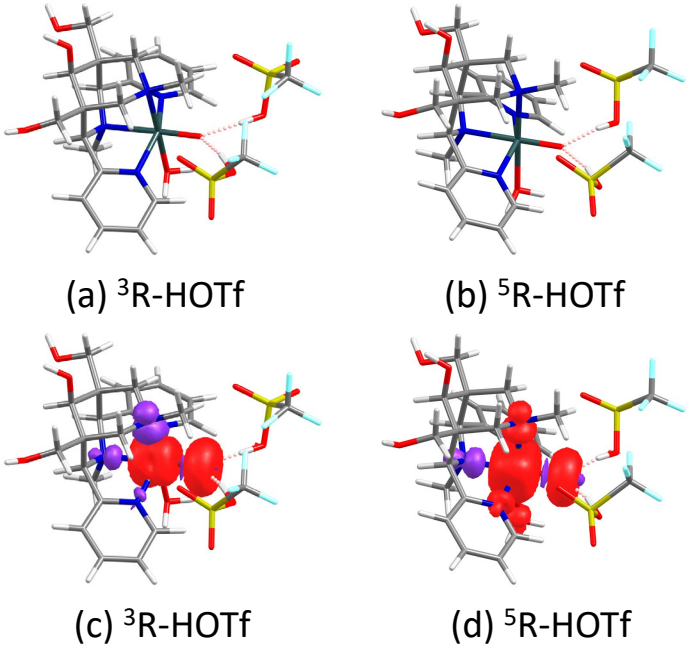

Fig. S27: Optimized geometries (a-b) and spin density plots (c-d) of OSET mechanism for ^{3}R-HOTf and ^{5}R-HOTf.

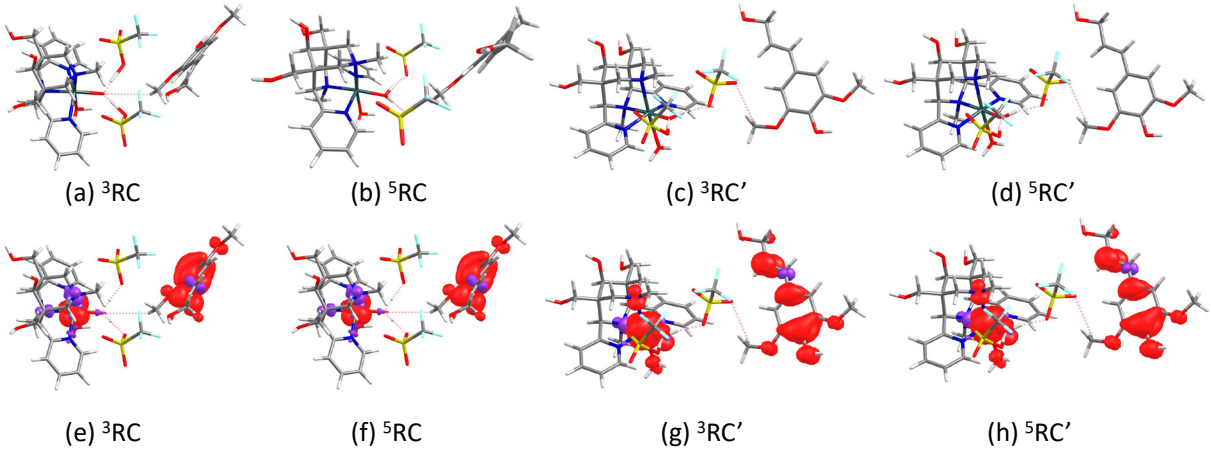

Fig. S28: Optimized geometries (a-d) and spin density plots (e-h) of OSET mechanism for ^{3}RC, ^{5}RC, ^{3}RC' and ^{5}RC'.

References

1. Hädeler, J. *et al.* Natural Abiotic Iron-Oxido-Mediated Formation of C1 and C2 Compounds from Environmentally Important Methyl-Substituted Substrates. *J. Am. Chem. Soc.* **145**, 24590-2460210.1021/jacs.3c06709 (2023).
2. Zeisel, S. ber ein Verfahren zum quantitativen Nachweise von Methoxyl. *Monatshefte fr Chemie* **6,** 989–997; 10.1007/bf01554683 (1885).
3. Page, S. E., Sander, M., Arnold, W. A. & McNeill, K. Hydroxyl radical formation upon oxidation of reduced humic acids by oxygen in the dark. *Environ. Sci. Technol* **46,** 1590–1597; 10.1021/es203836f (2012).
4. Zhang, N. *et al.* Dependence of Biotic and Abiotic H2O2 and •OH Production on the Redox Conditions and Compositions of Sediment during Oxygenation. *Environ. Sci. Technol* **58,** 3849–3857; 10.1021/acs.est.3c10424 (2024).
5. Page, S. E. *et al.* Dark formation of hydroxyl radical in Arctic soil and surface waters. *Environ. Sci. Technol* **47,** 12860–12867; 10.1021/es4033265 (2013).
6. Vermilyea, A. W., Dixon, T. C. & Voelker, B. M. Use of H2(18)O2 to measure absolute rates of dark H2O2 production in freshwater systems. *Environ. Sci. Technol* **44,** 3066–3072; 10.1021/es100209h (2010).
7. Schwertmann, U. Solubility and dissolution of iron oxides. *Plant Soil* **130,** 1–25; 10.1007/BF00011851 (1991).